Dalton Transactions

PAPER

View Article Online
View Journal

Cite this: DOI: 10.1039/c4dt03789h

Raman studies of A_2MWO_6 tungstate double perovskites†

R. L. Andrews, A. M. Heyns and P. M. Woodward*

Received 10th December 2014,
Accepted 23rd January 2015

DOI: 10.1039/c4dt03789h

www.rsc.org/dalton

The Raman spectra of seven A_2MWO_6 tungstate double perovskites are analysed. Ba_2MgWO_6 is a cubic double perovskite with $Fm\bar{3}m$ symmetry and its Raman spectrum contain three modes that can be assigned in a straightforward manner. A fourth mode, the asymmetric stretch of the $[WO_6]^{6-}$ octahedron, is too weak to be observed. The symmetry of Ba_2CaWO_6 is lowered to tetragonal $I4/m$ due to octahedral tilting, but the distortion is sufficiently subtle that the extra bands predicted to appear in the Raman spectrum are not observed. The remaining five compounds have additional octahedral tilts that lower the symmetry to monoclinic $P2_1/n$. The further reduction of symmetry leads to the appearance of additional lattice modes involving translations of the A-site cations and librations of the octahedra. Comparing the Raman spectra of fourteen different A_2MWO_6 tungstate double perovskites shows that the frequency of the symmetric stretch (ν_1) of the $[WO_6]^{6-}$ octahedron is relatively low for cubic perovskites with tolerance factors greater than one due to underbonding of the tungsten and/or M cation. The frequency of this mode increases rapidly as the tolerance factor drops below one, before decreasing gradually as the octahedral tilting gets larger. The frequency of the oxygen bending mode (ν_5) is shown to be dependent on the mass of the A-site cation due to coupling of the internal bending mode with external A-site cation translation modes.

Introduction

The perovskite family is one of the largest and most important in all of solid state chemistry. Perovskites have a stoichiometry of AMO_3, and the aristotype structure possesses $Pm\bar{3}m$ space group symmetry. The M cation resides at the centre of an octahedron, and the A cation occupies the cubooctahedral cavities that exist in the corner connected framework of MO_6 octahedra. Ordering of two unique octahedral cations on a three dimensional checkerboard pattern (*i.e.* rock salt ordering) leads to the $A_2MM'O_6$ double perovskite structure, where the unit cell is doubled along all three axes and the space group symmetry becomes $Fm\bar{3}m$. Double perovskites are a large group of compounds numbering more than 1000.[1–3] They are prized for a variety of properties and are used as relaxor ferroelectrics,[4] microwave dielectrics,[5] ionic conductors,[6] and half-metallic conductors.[7]

Most perovskites do not adopt the aristotype cubic structure, but are distorted in some manner. The most common type of distortion in perovskites is octahedral tilting.[2,3,8–10] When the tolerance factor is less than one, the size of the A-site cation is too small for its cuboctahedral cavity and cooperative tilts of essentially rigid octahedra are expected. Octahedral tilting modifies the coordination environment of the A-site cation while maintaining the octahedral coordination environment of the M and M′ cations. At the same time it lowers the overall symmetry of the crystal structure.

There are many examples in the literature of incorrect structure determinations that stem from an inability to correctly identify the correct pattern of octahedral tilting. This is particularly true for double perovskites because the diffraction peaks that arise from rock salt ordering of M and M′ ions are the same as those that arise from out-of-phase tilting of the octahedra.[11,12] In some instances neutron diffraction studies are needed to make definitive space group assignments, which can be problematic because access to neutron scattering facilities is limited.

Raman spectroscopy is an alternative technique for monitoring the reduction in symmetry that accompanies octahedral tilting. In theory additional bands should appear as the symmetry is lowered, but in practice it is not always possible to see all of the additional bands in spectra taken on polycrystalline samples. In this paper Raman spectroscopy is used to probe the local structure of seven $A_2M^{2+}WO_6$ double perovskites. The compounds studied were chosen to meet several criteria. By

Department of Chemistry and Biochemistry, The Ohio State University, 100 W. 18th Avenue, Columbus, OH 43210-1106, USA. E-mail: woodward.55@osu.edu

† Electronic supplementary information (ESI) available: Lattice parameters determined from Rietveld refinements of X-ray powder diffraction data, values of ν_1 and ν_5 modes for A_2MWO_6 perovskites studied in the literature, and Raman spectra of AWO_4 scheelite phases. See DOI: 10.1039/c4dt03789h

choosing perovskites whose tolerance factors range from 1.038 (Ba_2MgWO_6) to 0.867 (Ca_2CaWO_6) the group contains compounds with various patterns of octahedral tilting. Because the oxidation states of the M and M′ ions differ by four, the presence of antisite disorder, which can complicate interpretation of Raman spectra, can be avoided. By systematically analysing the Raman spectra of these compounds the links between changes in crystallographic symmetry and the appearance of new bands in the Raman spectra are revealed. By limiting the study to a set of perovskites where the strongest bonding unit, the $[WO_6]^{6-}$ octahedron, remains constant we can study the effect of changes in composition, bonding, and structure on the frequencies and intensities of the internal vibrations of the $[WO_6]^{6-}$ octahedron.

Experimental

All samples were prepared using conventional solid state synthesis methods. High purity (>99%) starting materials of $BaCO_3$, $SrCO_3$, CdO, MgO, ZnO, $CaCO_3$, and WO_3 were used. Stoichiometric amounts of the starting materials were ground in an agate mortar and pestle before heating in ceramic crucibles for 12–24 hours. Multiple heating cycles with intermittent grinding were necessary for some materials. The annealing temperature was 950 °C for Sr_2CdWO_6, 1000 °C for Sr_2ZnWO_6, 1200 °C for Ca_2CaWO_6, and 1300 °C for the remaining compounds. X-ray powder diffraction patterns were collected with a Bruker D8 Advance X-ray diffractometer (40 kV, 50 mA, copper source λ = 1.5406 Å). Rietveld refinements of the X-ray diffraction data were performed using Topas Academic software.[13] All Raman studies were performed using a Renishaw Smith Raman IR microprobe with a 514 nm Argon ion laser.

In some samples a few percent of an AWO_4 (A = Sr, Ba) secondary phase was detected by X-ray diffraction. To identify any peaks in the Raman spectra that come from the scheelite phases, phase pure samples of $BaWO_4$, $SrWO_4$ and $CaWO_4$ were synthesized following the same conventional solid state synthesis method with an annealing temperature of 1100 °C. The Raman spectra of the scheelite tungstates are given in the ESI.†

Results

Crystal structures

Throughout this paper octahedral tilting will be described using the notation developed by Glazer.[14] The $a^0a^0a^0$ tilt system is the aristotype cubic structure with $Fm\bar{3}m$ space group symmetry, while the other three tilt systems encountered in tungstate double perovskites are illustrated in Fig. 1.

The tilt systems reported in the literature, both at ambient conditions and as a function of temperature, are summarized in Table 1. There is some controversy regarding assignment of tilt systems in Ba_2CaWO_6. Yamamura *et al.* assigned the 220 K

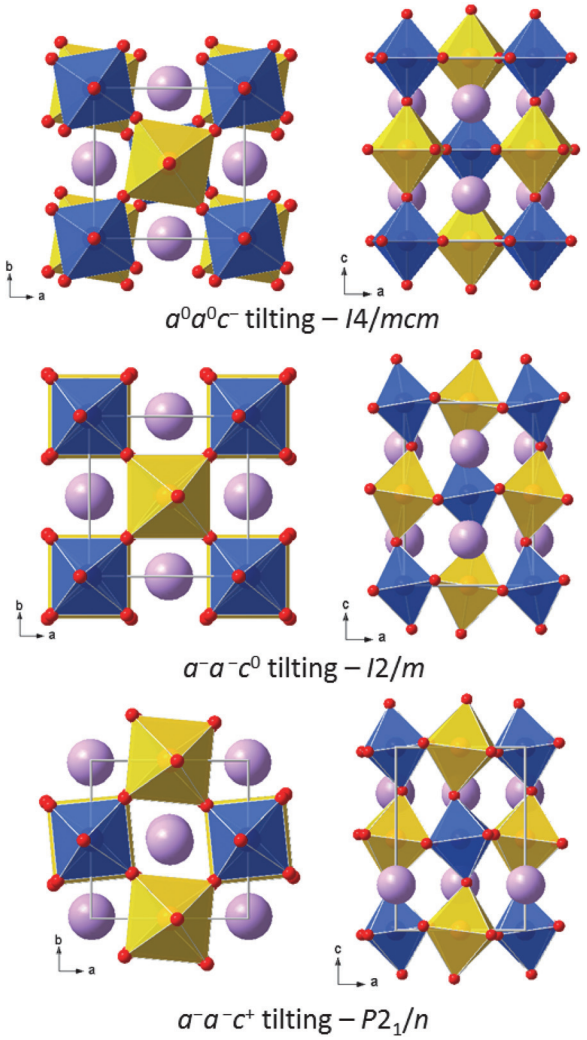

Fig. 1 The structure of a double perovskite with $a^0a^0c^-$ (upper), $a^0b^-b^-$ (middle), and $a^-a^-b^+$ (lower) tilting.

Table 1 The tolerance factors, tilt system at 300 K, and phase transitions that have been identified in the A_2MWO_6 perovskites under study

Composition	Tolerance factor (t)	Octahedral tilting
Ba_2MgWO_6 [17]	1.038	$a^0a^0a^0$ (at 300 K)
Sr_2ZnWO_6 [17]	0.976	$a^-a^-c^+ \xrightarrow{343\ K} a^0a^0c^-$
Ba_2CaWO_6 [15,17]	0.972	$a^-a^-c^0 \xrightarrow{220\ K} a^0a^0c^-$
Sr_2CdWO_6 [18,19]	0.930	$a^-a^-c^+ \xrightarrow{1070\ K} a^0a^0c^- \xrightarrow{1230\ K} a^0a^0a^0$
Ca_2MgWO_6 [20]	0.926	$a^-a^-c^+$ (at 300 K)
Sr_2CaWO_6 [19]	0.917	$a^-a^-c^+ \xrightarrow{1130\ K} a^0a^0c^- \xrightarrow{1250\ K} a^0a^0a^0$
Ca_2CaWO_6 [17]	0.867	$a^-a^-c^+$ (at 300 K)

phase transition as being driven by a change from monoclinic $I2/m$ symmetry ($a^-a^-c^0$ tilting) to tetragonal $I4/m$ symmetry ($a^0a^0c^-$ tilting),[15] while Fu *et al.* claimed the transition was actually from $I4/m$ symmetry to cubic $Fm\bar{3}m$ symmetry ($a^0a^0a^0$ tilting).[16] Day *et al.* later investigated the room temperature structure using both X-ray and neutron diffraction and

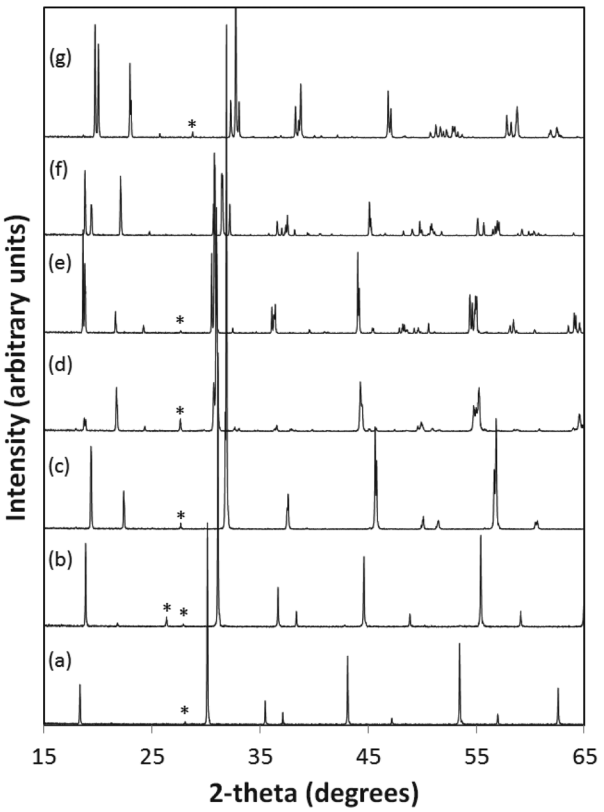

Fig. 2 X-ray diffraction patterns of (a) Ba_2CaWO_6, (b) Ba_2MgWO_6, (c) Sr_2ZnWO_6, (d) Sr_2CdWO_6, (e) Sr_2CaWO_6, (f) Ca_2CaWO_6 and (g) Ca_2MgWO_6. The peak splitting that results from octahedral tilting can clearly be seen in (c) through (g). The strongest peaks due to the secondary AWO_4 scheelite phases are marked with an asterisk.

concluded that the symmetry at room temperature was tetragonal $I4/m$.[17] Therefore, the assignment originally put forward by Yamamura *et al.* seems most credible and is given in Table 1. However, there is a possibility that the symmetry of this compound might be sample dependent.

The X-ray diffraction patterns illustrating the phase purity and peak splitting characteristic associated with various types of octahedral tilting are shown in Fig. 2. Rietveld refinements yielded lattice parameters that are in good agreement with those already reported in the literature, as shown in the ESI (Table S1†).[15,17–20] The atomic coordinates for six of the seven compounds have previously been determined from neutron powder diffraction data, thus the values obtained in our refinements are not reported here. The lone exception is Sr_2CdWO_6, where the high neutron absorption cross section of cadmium makes neutron diffraction studies impractical. The refined atomic positions for Sr_2CdWO_6 can be found in Table 2 and the refined diffraction pattern is shown in Fig. 3. The monoclinic symmetry and atomic coordinates are in good agreement with those reported by Gateshki *et al.*[18]

During the synthesis of these particular tungsten based perovskites, it was difficult to completely eliminate all traces of a scheelite ($A^{2+}WO_4$) secondary phase, as can be seen by close inspection of Fig. 2. Most samples contained less than 1% by

Table 2 Refined atomic positions for Sr_2CdWO_6 as obtained from Rietveld refinement of powder diffraction data. The goodness of fit was χ^2 = 1.148

Atom	Site	x	y	z	$B_{eq.}$ [a]
Sr	4e	0.0074(4)	0.5371(9)	0.2520(5)	0.577(7)
Cd	2c	0.5	0.5	0	0.402(9)
W	2d	0	0	0	0.402(9)
O1	4e	0.0700(9)	0.0142(5)	−0.2312(5)	1.003(0)
O2	4e	0.2604(9)	−0.1883(2)	0.0300(2)	1.003(0)
O3	4e	0.1812(5)	0.2665(4)	0.0444(0)	1.003(0)

[a] The $B_{eq.}$ values for Cd and W were constrained to be the same, as were the $B_{eq.}$ values of O1, O2, and O3.

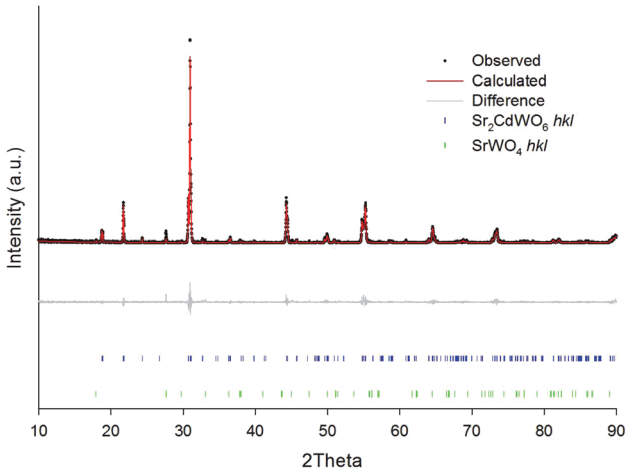

Fig. 3 Rietveld refinement of Sr_2CdWO_6. The upper (blue) and lower (green) set of hash marks, denote the position of the Sr_2CdWO_6 and $SrWO_4$ reflection positions, respectively.

mass, but Sr_2MgWO_6 and Sr_2CdWO_6 had approximately 3% and 2% by mass, respectively. The presence of AWO_4 crystallites at such low levels is not likely to impact the crystallography in any meaningful way. However, it is important to identify these phases because as will be seen later, weak bands associated with the scheelite phases are observed in many of the Raman spectra.

To better understand how changes in structure impact the Raman spectra that will be presented in the next section the M–O–W bond angles, mean octahedral bond lengths, and distortion indices Δ_d are reported in Table 3. The distortion index (Δ_d) measures the degree to which the M–O and W–O bond distances are distorted from those found in a perfect octahedron. The distortion index is calculated as follows:

$$\Delta_d = \frac{1}{6}\sum_{n=1-6}\left[\frac{d_n - < d >}{< d >}\right]^2$$

where d_n is an individual M–O bond length and <d> is the average M–O bond length. Octahedra with significant distortions of the bond lengths (*e.g.* those containing Jahn Teller ions like Mn^{3+}) have Δ_d values greater than 10^{-3}.[17,22] As can be seen in Table 3 the values of Δ_d are generally quite small here,

Table 3 Select bond distances, bond angles and octahedral distortion indices for the A_2MWO_6 perovskites under study. All parameters determined from previous neutron powder diffraction studies, with the exception of Sr_2CdWO_6

Composition	Mean M–O distance (Å)	M^{2+} distortion index ($\times 10^5$)	Mean W–O distance (Å)	W^{6+} distortion index ($\times 10^5$)	M–O–W bond angles (°)
Ba_2MgWO_6 [17]	2.123	0	1.929	0	180
Sr_2ZnWO_6 [17]	2.084	0.16	1.918	0.11	167.6
					165.4
					164.1
Ba_2CaWO_6 [17]	2.281	2.3	1.920	3.5	180
					176.0
Sr_2CdWO_6	2.274	22	1.899	15	157.1
					158.5
					152.1
Ca_2MgWO_6 [20]	2.069	1.1	1.922	1.9	152.3
					151.1
					152.1
Sr_2CaWO_6 [21]	2.339	6.6	1.911	2.5	153.9
					149.1
					147.1
Ca_2CaWO_6 [17]	2.304	12	1.926	1.4	147.2
					140.9
					141.4

confirming the picture that these structures can be described by tilts of nearly rigid octahedra. The largest distortion occurs in Sr_2CdWO_6, but given the larger uncertainties associated with determining the structure using laboratory X-ray diffraction it's quite possible that the values of Δ_d are overestimated in Sr_2CdWO_6. The next largest distortion occurs for the Ca-centered octahedra in Ca_2CaWO_6 ($\Delta_d = 1.16 \times 10^{-4}$). This distortion is also present in the internal bond angles of the calcium octahedron: O1–Ca–O3 = 94.83° and O2–Ca–O3 = 95.08°. According to Day *et al.*, this can be attributed to the large octahedral tilting distortion and relatively ionic Ca–O bonds, conditions where the assumption of cooperative tilting of truly rigid octahedra starts to break down.[17]

The average W–O distance is fairly constant for all seven compounds, as would be expected, with Sr_2CdWO_6 once again showing up as somewhat of an outlier. The M–O–W bond angles, which are linear in the cubic perovskite structure, become increasingly bent as the tolerance factor decreases and the octahedral tilting becomes more pronounced. The fact that the Ca–O2–W bond in Ba_2CaWO_6 is nearly linear indicates that this compound is on the verge of a phase transition to the undistorted $Fm\bar{3}m$ structure.

Raman spectra of Ba_2MWO_6 (M = Ca, Mg) double perovskites

Group theory analysis for a double perovskite with the aristotype cubic $Fm\bar{3}m$ structure shows that there are four Raman active bands expected, $\Gamma = \nu_1(A_{1g}) + \nu_2(E_g) + \nu_5(F_{2g}) + T(F_{2g})$, where ν_1, ν_2, and ν_5 are the internal vibration modes of an octahedron and T is a lattice mode. The ν_1 mode is the symmetric oxygen stretch vibration of the octahedra, during which all cations are at rest and the oxygen atoms are moving along the M–O–W axis.[23] It appears as a strong, relatively broad peak in the region of 750–850 cm^{-1}.[23,24] Just as there is an oxygen symmetric stretch, there is also an oxygen asymmetric stretching vibration, labelled as the ν_2 mode. Again, during a ν_2 vibration, all cations are at rest while the oxygen atoms vibrate along the M–O–W axes.[23] The internal ν_5 mode is due to an oxygen bending motion of the octahedron. The ν_2 and ν_5 modes are expected to occur in the ranges 470–610 cm^{-1} and 350–490 cm^{-1} respectively.[23,24]

Low energy lattice modes can be classified as external modes (*i.e.* not associated with the internal vibration of an octahedron).[25] The external T modes found in the 100–300 cm^{-1} region arise from translations of the A cation, and are referred to as translational lattice modes.[23] The librational modes, L, which are also considered lattice modes, can be described as rotations of rigid octahedra. When the crystal has $Fm\bar{3}m$ symmetry, as Ba_2MgWO_6 does, the librational mode of F_{1g} symmetry is silent and there is a single Raman active translational mode, $T(F_{2g})$.

In the Raman spectrum of Ba_2MgWO_6 (see Fig. 4), the peaks at 126, 441, and 812 cm^{-1} are assigned to $T(F_{2g})$, $\nu_5(F_{2g})$, and $\nu_1(A_{1g})$ modes, respectively. The ν_2 asymmetric stretching mode is too weak to be seen, but is calculated to occur at 540–550 cm^{-1} in normal coordinate calculations using a Urey-Bradley force field. Its intensity is likewise calculated to be approximately 8% of the $\nu_1(A_{1g})$ mode. As we will see a very weak ν_2 mode is not unusual for these ordered double perovskites. These values and assignments are in good agreement with those reported by Liegeois-Duyckaerts and Tarte.[23]

When lowering the symmetry to $I4/m$, as is the case for Ba_2CaWO_6, additional Raman bands are allowed. The irreducible representation, considering only Raman active vibrations, for a double perovskite with $I4/m$ symmetry is $\Gamma = \nu_1(A_g) + \nu_2(A_g + B_g) + \nu_5(B_g + E_g) + T(B_g + E_g) + L(A_g + E_g)$, which corresponds to nine Raman active modes. However, as shown in Fig. 4, only three bands are visible with the lowest energy band falling at the extreme low energy range that can be accessed with our spectrometer. There are various reasons that could be responsible for the absence of extra bands predicted by group theory on lowering the symmetry from $Fm\bar{3}m$ to $I4/m$: (1) bands may be so weak that they are not detected above the background, (2) bands may overlap to such an extent that we are not able to

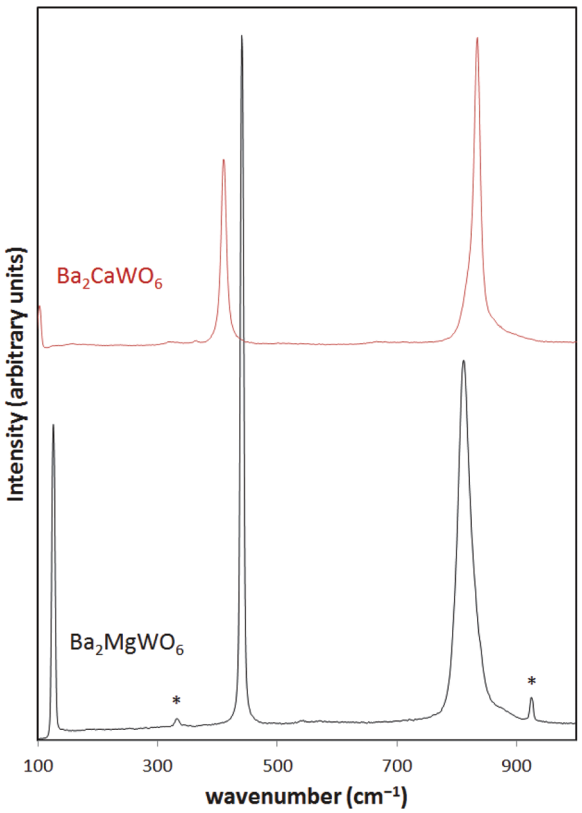

Fig. 4 Raman spectra of Ba_2MgWO_6 and Ba_2CaWO_6. The peaks marked with an asterisk are due to the scheelite phase $BaWO_4$.

resolve the splitting of the bands, or (3) new bands may fall at energies lower than 100 cm^{-1}.

The bands appearing at approximately 834, 410, and 103 cm^{-1} can be assigned to ν_1, ν_5, and T modes respectively for Ba_2CaWO_6, although there is some uncertainty in the frequency of the band seen at 103 cm^{-1} because it falls at the very edge of the accessible range of our spectrometer. As was the case for Ba_2MgWO_6 the asymmetric stretch, ν_2, is too weak to be observed. Furthermore, the predicted splitting of the ν_5 mode is too small to be resolved. This is presumably because the degree of distortion from the cubic structure is quite small in Ba_2CaWO_6, (see the bond angles and distances in Table 3). The libration modes L and the additional T mode are either too weak to see or fall outside of the spectral range of our spectrometer. Liegeois-Duyckaerts and Tarte observed very similar bands (838, 413, 105 cm^{-1}) and from the presence of just three Raman bands concluded that Ba_2CaWO_6 was cubic.[23] However, as discussed above careful diffraction studies later showed that the true symmetry was tetragonal $I4/m$.[15,17] So in this case it appears that Raman spectroscopy is no more sensitive, perhaps less so, than X-ray powder diffraction for detecting the subtle lowering in symmetry.

Raman spectra of monoclinic A_2MWO_6 double perovskites

The remaining five compounds have additional octahedral tilting distortions (tilt system $a^-a^-b^+$) that lower the symmetry to the monoclinic space group $P2_1/n$. Considering only Raman active modes, the irreducible representation for a $P2_1/n$ perovskite can be written as $\Gamma = \nu_1(A_g + B_g) + \nu_2(2A_g + 2B_g) + \nu_5(3A_g + 3B_g) + T(3A_g + 3B_g) + L(3A_g + 3B_g)$. There are now a total of 24 bands predicted to be present in the Raman spectrum, however, in the five compounds studied here only seven to thirteen bands are experimentally observed (see Table 4). In these structures there are two A_2MWO_6 formula units per unit cell, and this leads to the presence of A_g and B_g components for all of the modes. It would not be unexpected if the A_g and B_g components of the internal modes fell at a very similar frequencies, in which case polarized Raman spectra of single crystals may be needed to resolve them. If that is the case spectra collected on polycrystalline samples, as is the case here, should exhibit a single band for the symmetric stretch ν_1, a doublet for the asymmetric stretch ν_2, and a triplet for the bending mode ν_5.

The Raman spectra of the monoclinic double perovskites are shown in Fig. 5. An intense oxygen symmetric stretch band, ν_1, is seen in each spectrum at values ranging from 811 to 855 cm^{-1}. Unlike Ba_2CaWO_6 and Ba_2MgWO_6, the oxygen asymmetric stretching mode, ν_2, can be seen in these compounds, but it is so weak that it's not possible to detect splitting of this band without polarized Raman data. The peak

Table 4 Raman shifts (in cm^{-1}) for the observed modes in the tungsten double perovskites with $P21/n$ symmetry

Assignment	Sr_2ZnWO_6	Sr_2CdWO_6	Sr_2CaWO_6	Ca_2MgWO_6	Ca_2CaWO_6
T	137	129	110	149	132
T	152	151	126	165	144
T	170	172	134	176	193
T	—	190	150	192	207
T	—	—	173	212	218
T	—	—	195	—	—
L	—	246	—	249	247
L	—	—	—	304	256
L	—	—	—	330	301
ν_5 or L	—	390	395	406	—
ν_5 or L	—	411	415	424	416
ν_5	436	440	441	472	453
ν_5	445	465	465	—	465
ν_2	573	554	583	584	594
ν_1	855	824	818	836	811
AWO_4	921	921, 800, 371, 336	922	908, 331	—

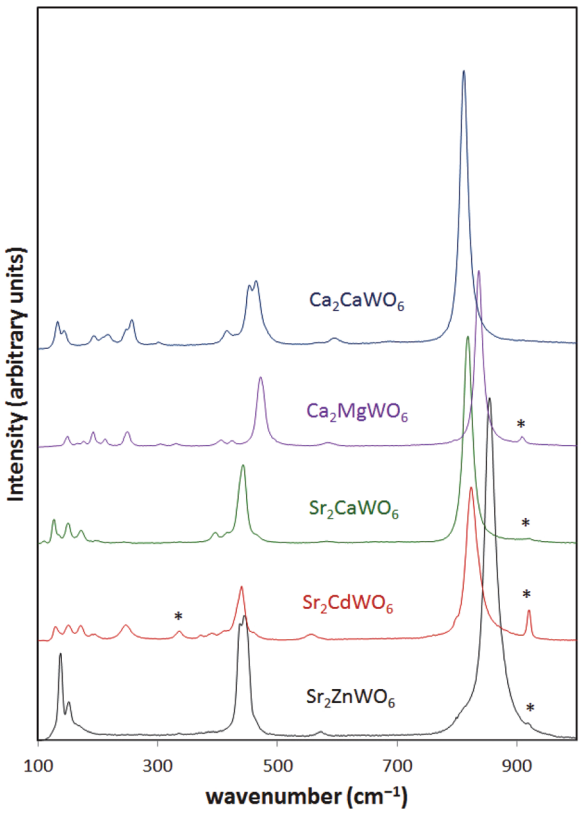

Fig. 5 Raman spectra of five tungsten-based perovskites with space group $P2_1/n$. The peaks marked with an asterisk are due to the scheelite secondary phase, either $SrWO_4$ or $CaWO_4$.

at approximately 918 cm^{-1} in the Sr_2CdWO_6 spectrum is assigned to $SrWO_4$. Not only is this where the strongest band in the Raman spectrum of $SrWO_4$ is observed (see ESI†), the presence of a peak from the secondary scheelite phase is not unexpected given the presence of $SrWO_4$ in the XRD pattern of Sr_2CdWO_6. Very weak AWO_4 scheelite peaks can also be seen in the spectra of several other compounds.

The internal oxygen bending motion, ν_5 that falls between 400–500 cm^{-1} is the second strongest set of peaks in the spectra. If the A_g and B_g components cannot be resolved then the ν_5 mode is expected to split into a triplet. As shown in Fig. 5, the ν_5 mode is clearly split into a doublet in Sr_2ZnWO_6 and Ca_2CaWO_6. The splitting is more difficult to resolve in the other three compounds. Why the splitting should be seen most easily in the compounds that have the largest and smallest tolerance factors of the group, respectively, is not clear.

Proceeding to lower wavenumbers, the libration lattice modes are the next peaks expected to appear. In a perovskite with $P2_1/n$ symmetry, six libration lattice modes are predicted, three A_g and three B_g modes. Sr_2ZnWO_6 does not appear to have any librational modes that are strong enough to be seen above the background. Lentz reported peaks in this area of the spectrum in his study of Sr_2ZnWO_6, but they were extremely weak, thus explaining the absence of visible libration modes in our spectra.[26] Sr_2CdWO_6, Ca_2MgWO_6 and Ca_2CaWO_6 all have a peak of moderate intensity near 250 cm^{-1} that we assign as a libration mode L. Curiously this peak is too weak to be observed in Sr_2CaWO_6. Additionally most of the compounds have weak peaks between 390 and 420 cm^{-1} that cannot be unambiguously assigned as being either an external libration mode or an internal bending mode.

The translation lattice modes are expected at the lowest frequencies. In a perovskite with $P2_1/n$ symmetry, six translation lattice modes are predicted, *via* a triplet splitting of the A_g and B_g modes. Where the libration modes end and the translation modes begin is not completely clear. Polarized Raman and infrared spectra are needed to accurately differentiate libration and translation lattice modes. In a study of $A_2CoM'O_6$ (A = Sr, Ca; M′ = W, Te) Ayala *et al.* assigned the libration lattice modes to frequencies in the range 190–310 cm^{-1}, and translation lattice modes to frequencies less than 190 cm^{-1} for $P2_1/n$ double perovskites,[24] but as discussed below there is some evidence that the translation lattice modes may extend as high as 220 cm^{-1} in these compounds.

Lentz previously reported the Raman spectra for Sr_2ZnWO_6 (t = 0.976), which showed weak bands at 78, 105, and 116 cm^{-1}, the first of these is outside of the range of our spectrometer, while the latter two are not observed in this study. Lentz also observed modes at 140 and 153 cm^{-1}, corresponding to the translational lattice modes that are observed here.[23] There is a broad tailing that occurs on the high frequency side of the doublet, centered approximately at 170 cm^{-1} and it is possible that this broad feature may correspond to a third translational mode. Looking back at Table 3, the Zn–O–W angles range from 164° to 168°, which are the least bent of all the $P2_1/n$ perovskites considered here. It could be argued that the relatively small magnitude of octahedral tilting leads to less splitting of the translational modes in this compound than the other $P2_1/n$ perovskites. The close proximity to the $P2_1/n \rightarrow I4/m$ phase transition at 343 K (see Table 1) may also play a role in making the splitting of the translational modes too subtle to resolve.

Sr_2CdWO_6 (t = 0.930) shows a definitive triplet splitting with peaks at 129, 151, 172 cm^{-1}, and a fourth very weak peak at 190 cm^{-1}. The lower tolerance factor leads to more distorted Cd–O–W bonds, with angles that range from 152° to 159°. Sr_2CaWO_6, which has the same A-site cation and a similar tolerance factor (t = 0.916), has four translational modes that fall at nearly the same wavenumbers, as well as additional weak peaks at 110 and 134 cm^{-1}. These values are in good agreement with those reported by Gateshki and Igartua.[27]

Coming to Ca_2MgWO_6 the tolerance factor lies in the same range (t = 0.926) but the A-site cation is now Ca^{2+} instead of Sr^{2+}. Since the translational modes involve motions of the A-site cation the lighter mass of the Ca^{2+} ion (40.1 *vs.* 87.6 amu) should result in a shift of these modes to higher frequencies. Based on that expectation five peaks between 149 and 212 cm^{-1} are tentatively assigned as translational modes. If this assignment is correct the modes shift to higher frequencies by 20 to 40 cm^{-1} when Sr^{2+} is replaced by Ca^{2+}.

Finally, Ca_2CaWO_6, which has the smallest tolerance factor (t = 0.867) and more highly bent M–O–W bonds (141° to 147°), also appears to have five translational modes that fall in a

similar region of the spectrum, but the increased distortion of the structure leads to clear differences in the intensities and frequencies of these modes with respect to Ca_2MgWO_6.

Preliminary results obtained from force constant calculations show that considerable coupling occurs between the lower-lying wavenumber bands of these solids. Unfortunately because they are both weak and numerous unambiguous assignments cannot be made without the availability of single crystal Raman and infrared data.

Discussion

The frequency of the symmetric stretch, ν_1, is plotted as a function of tolerance factor in Fig. 6 for the seven compounds studied here, as well as an additional seven A_2MWO_6 double perovskites—Ba_2NiWO_6,[23] Ba_2ZnWO_6[23] Ba_2MnWO_6,[28] Sr_2MgWO_6,[29] Sr_2CoWO_6,[24] Sr_2MnWO_6,[28] and Ca_2CoWO_6.[24] The tolerance factors and frequencies of the ν_1 and ν_5 bands for these additional compounds are given in the ESI (Table S2†). The frequency of the ν_1 mode does not appear to be very sensitive to the identity of the A cation, nor to the mass of the M cation, as expected for an internal mode of the octahedron that does not involve motion of the cations. However, it does show a dependence on the tolerance factor.

The cubic double perovskites with tolerance factors larger than one have relatively low frequency symmetric stretches (810–822 cm^{-1}). Once the tolerance factor drops below one and octahedral tilting distortions set in, the frequency of the ν_1 mode spikes. This result can be understood in the following manner. In those A_2MWO_6 double perovskites where the tolerance factor is larger than one, the octahedra are stretched by the oversized A-site cation. This effect weakens the M–O and/or the W–O bonds, thereby lowering the energy of the oxygen ion vibration along the M–O–W axis.

To support this hypothesis consider Table 5, which contains the bond valence sums for each of the five Ba_2MWO_6 compounds included in Fig. 6. Only in Ba_2CaWO_6 (t = 0.972) does the bond valence sum of tungsten exceed its ideal value of 6, and the Ca^{2+} ion is also overbonded in this compound. Despite the tetragonal symmetry the bonds are still quite close to linear in this compound (see Table 3). Given the fact that both the M–O and W–O bonds are effectively compressed from their ideal values, it should not come as a surprise that the position of the symmetric stretch is 12–22 cm^{-1} higher than it is in the other Ba_2MWO_6 compositions.

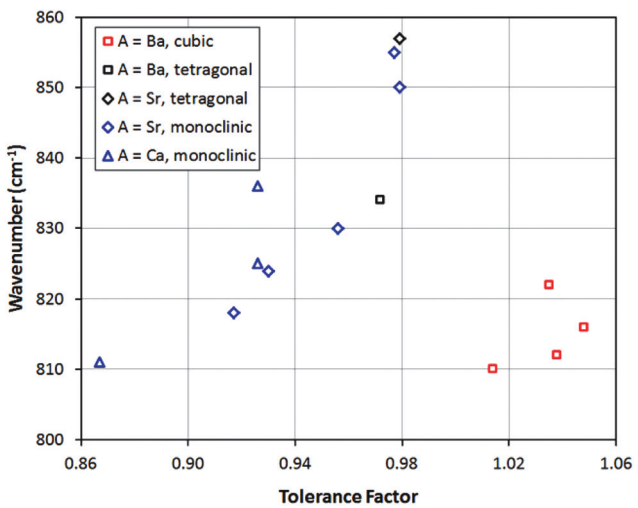

Fig. 6 Frequencies of the oxygen symmetric stretch ν_1 as a function of tolerance factor for A_2MWO_6 double perovskites.

Table 5 Tolerance factor, symmetric stretching frequency, and bond valence sums for Ba_2MWO_6 double perovskites

Compound	Tolerance factor	ν_1 (cm^{-1})	Bond valence sums			
			Ba	M^{2+}	W	O
Ba_2NiWO_6	1.048	816	2.58	1.81	5.70	2.11
Ba_2MgWO_6	1.038	812	2.49	1.88	5.87	2.12
Ba_2ZnWO_6	1.035	822	2.45	1.87	5.88	2.11
Ba_2MnWO_6	1.014	810	2.27	2.11	5.90	2.09
Ba_2CaWO_6	0.972	834	1.87	2.57	6.02	2.06

Once octahedral tilting has set in a further decrease in the tolerance factor leads to a decrease in the energy of the ν_1 symmetric stretching mode. This trend can also be rationalized by taking into account how the structure changes as the tolerance factor continues to decrease. Because the W–O bonds are easily the strongest bonds in these compounds the internal ν_1 mode can be thought of as a vibration of the $[WO_6]^{6-}$ octahedra. When the W–O–M bonds are linear an expansion in the W–O bond leads to an equivalent compression of the M–O bonds, and *vice versa*. However, as the tolerance factor decreases the M–O–W bonds become increasingly bent. Once the W–O–M bonds are bent an expansion of the bonds in each $[WO_6]^{6-}$ octahedron does not lead to a pure compression of the M–O bonds, but rather a mixture of compression and bending. As a general rule bending modes are lower energy than stretching modes, hence there is less resistance to changes in the W–O bond lengths when the M–O–W bonds are bent.

Plotting the frequencies of the ν_5 bending mode tells a different story, as shown in Fig. 7. The frequencies for double perovskites with A = Sr cluster into a narrow range of values that fall between 439–450 cm^{-1}. The frequency of the bending mode shifts to higher values when A = Ca, and lower values when A = Ba. The relative order ν_5(A = Ba) < ν_5(A = Sr) < ν_5(A = Ca) mirrors the relative masses of the three A-site cations, and is a clear sign that a motion of the A-site cation must also be involved in the oxygen bending mode. Returning to the group theory discussed earlier we see that this coupling of internal and external modes is allowed because the oxygen bending mode and the A-site cation translation mode have one or more common irreducible representations for all three space group symmetries. Thus it is not completely accurate to describe this mode as a pure internal vibration of the octahedron.

The frequency of the ν_5 mode for the Ba-containing double perovskites shows some dependence on tolerance factor. Once again the bond valence sums shown in Table 5 are illustrative. Because the oxygen bending mode leads to changes in the A–O

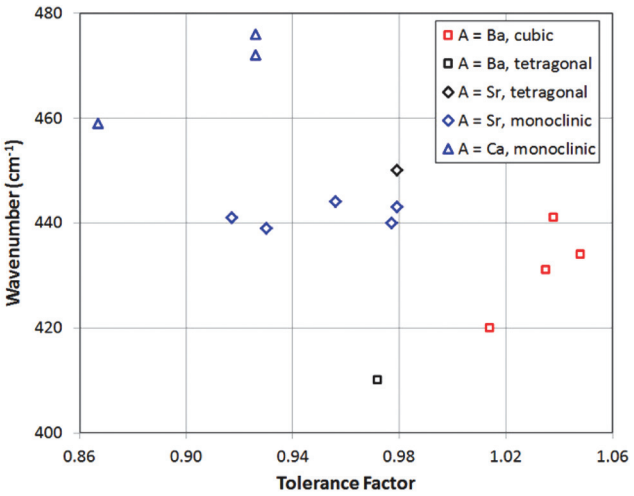

Fig. 7 Frequencies of the oxygen bending mode ν_5 as a function of tolerance factor for A_2MWO_6 double perovskites.

bond lengths, its frequency should increase as the Ba^{2+} ion becomes increasingly overbonded. Table 5 and Fig. 7 show that as the tolerance factor increases so does the valence of the Ba^{2+} ion and hence the frequency of the ν_5 mode.

Conclusions

As the symmetry is lowered from cubic $Fm\bar{3}m$ to monoclinic $P2_1/n$ additional peaks appear in the Raman spectrum, as predicted by group theory. However, it is not possible to observe/resolve all 24 peaks that are predicted in spectra taken on polycrystalline samples. The lone tetragonal $I4/m$ compound that was studied, Ba_2CaWO_6, did not exhibit any peaks in its Raman spectrum that would signal a lowering of the symmetry from cubic to tetragonal. The frequency of the oxygen symmetric stretch ν_1 is relatively low for cubic perovskites with tolerance factors larger than one, but increases sharply as the tolerance factor drops below one and octahedral tilting sets in ($t \approx 0.98$). Further decreases in tolerance factor lead to a gradual decrease in the frequency of the ν_1 mode. The frequency of the oxygen bending mode ν_5 increases as the mass of the A cation decreases. This observation is clear evidence that the ν_5 vibrational mode of the $[WO_6]^{6-}$ octahedron, strongly couples to one or more external lattice modes.

Acknowledgements

Financial support from the National Science Foundation (Award number DMR-0907356) is acknowledged.

Notes and references

1 M. T. Anderson, K. B. Greenwood, G. A. Taylor and K. R. Poeppelmeier, *Prog. Solid State Chem.*, 1993, **22**, 197.
2 M. W. Lufaso, P. W. Barnes and P. M. Woodward, *Acta Crystallogr., Sect. B: Struct. Sci.*, 2006, **62**, 397.
3 S. Vasala and M. Karppinen, *Prog. Solid State Chem.*, 2014, **42**, 1.
4 A. A. Bokov and Z.-G. Ye, *J. Mater. Sci.*, 2006, **41**, 31.
5 A. Dias, G. Subodh, M. T. Sebastian and R. L. Moreira, *J. Raman Spectrosc.*, 2010, **41**, 702.
6 J. B. Goodenough and Y. H. Huang, *J. Power Sources*, 2007, **173**, 1.
7 K. L. Kobayashi, T. Kimura, H. Sawada, K. Terakura and Y. Tokura, *Nature*, 1998, **395**, 677.
8 P. M. Woodward, *Acta Crystallogr., Sect. B: Struct. Sci.*, 1997, **53**, 44.
9 M. W. Lufaso and P. M. Woodward, *Acta Crystallogr., Sect. B: Struct. Sci.*, 2001, **57**, 725.
10 G. King and P. M. Woodward, *J. Mater. Chem.*, 2010, **20**, 5785.
11 P. W. Barnes, M. W. Lufaso and P. M. Woodward, *Acta Crystallogr., Sect. B: Struct. Sci.*, 2006, **62**, 384.
12 C. J. Howard, B. J. Kennedy and P. M. Woodward, *Acta Crystallogr., Sect. B: Struct. Sci.*, 2003, **59**, 463.
13 R. W. Cheary and A. Coelho, *J. Appl. Crystallogr.*, 1992, **25**, 109.
14 A. M. Glazer, *Acta Crystallogr., Sect. B: Struct. Crystallogr. Cryst. Chem.*, 1972, **28**, 3384.
15 K. Yamamura, M. Wakeshima and Y. Hinatsu, *J. Solid State Chem.*, 2006, **179**, 605.
16 W. T. Fu, Y. S. Au, S. Akerboom and D. J. W. IJdo, *J. Solid State Chem.*, 2008, **181**, 2523.
17 B. E. Day, N. D. Bley, H. R. Jones, R. M. McCullough, H. W. Eng, S. H. Porter, P. M. Woodward and P. W. Barnes, *J. Solid State Chem.*, 2012, **185**, 107.
18 M. Gateshki, J. M. Igartua and E. Hernandez-Bocanegra, *J. Phys.: Condens. Matter*, 2003, **15**, 6199.
19 A. Faik, J. M. Igartua and J. L. Pizarro, *J. Mol. Struct.*, 2009, **920**, 196.
20 J. H. Yang, W. K. Choo and C. H. Lee, *Acta Crystallogr., Sect. C: Cryst. Struct. Commun.*, 2003, **59**, 86.
21 G. Madariaga, A. Faik, T. Breczewski and J. M. Igartua, *Acta Crystallogr., Sect. B: Struct. Sci.*, 2010, **66**, 109.
22 J. A. Alonso, M. J. Martinez-Lopez, M. T. Casais and M. T. Fernandez-Diaz, *Inorg. Chem.*, 2000, **39**, 917.
23 M. Liegeois-Duyckaerts and P. Tarte, *Spectrochim. Acta, Part A*, 1974, **30**, 1771.
24 A. P. Ayala, I. Guedes and E. N. Silva, *J. Appl. Phys.*, 2007, **101**, 123511.
25 J. R. Ferraro; K. Nakamoto; and C. W. Brown, *Introductory Raman Spectroscopy*, Academic Press, New York, 2003.
26 V. A. Lentz, *Z. Anorg. Allg. Chem.*, 1973, **402**, 153.
27 M. Gateshki and J. M. Igartua, *J. Phys.: Condens. Matter*, 2004, **16**, 6639.
28 Y. Fujioka, J. Frantti and M. Kakihana, *J. Phys. Chem. B*, 2006, **110**, 777.
29 B. Manoun, A. Ezzahi, S. Benmokhtar, L. Bihc, Y. Tamraoui, R. Haloui, F. Mirinioui, S. Addakiri, J. M. Igartua and P. Lazor, *J. Mol. Struct.*, 2013, **1045**, 1.